Comprehensive Cost Optimization for Charger Deployment in Multi-hop Wireless Charging

Sixu Wu, Haipeng Dai, *Member, IEEE,* Lijie Xu, Linfeng Liu, *Member, IEEE,* Fu Xiao, *Member, IEEE,* Jia Xu, *Senior Member, IEEE*

Abstract—The multi-hop wireless charging technology can largely extend the charging service range of chargers, thus has promising prospect in sustainable energy replenishment for wireless rechargeable sensor network. This paper proposes a new cost criterion, termed comprehensive cost consisting of energy cost and deployment cost, to measure the actual expenditure of wireless charging. We present a multi-hop wireless charging model and formulate the problem of minimizing the comprehensive cost such that the energy demand of all sensor nodes can be fulfilled by the energy capacitated chargers. We propose a $(\ln n + 1)$-approximation algorithm for the optimization problem, where n is the number of sensor nodes. Then, we propose a straightforward cost sharing mechanism, which ensures that no subset of sensor nodes can benefit by breaking away from the current charging tree for any fixed charger position, to realize the paid charging service of multi-hop wireless charging. Furthermore, to keep the magnetic fields of transmitters from the interfering, the conflict avoidance schemes are proposed in both central and distributed situations. Finally, we discuss the distributed scheme for minimizing the comprehensive cost without support of central server. Through extensive simulations, we demonstrate the significant superiority of the proposed algorithms in terms of comprehensive cost.

Index Terms—wireless rechargeable sensor network, multi-hop wireless charging, magnetic resonance, charger deployment.

1 Introduction

With the development of wireless charging technology, Wireless Rechargeable Sensor Network (WRSN) has been widely applied in various fields, such as automobile, military target tracking and surveillance, natural disaster relief, biomedical health monitoring, and hazardous environment exploration [1]. The wireless charging technology largely determines the cost and efficiency of power transfer. So far, there have been many wireless charging technologies, such as magnetic resonance [2, 3], inductive coupling [4, 5], RF [6, 7], and microwave [8], which have different properties and are applicable for various scenarios.

Among these wireless charging technologies, magnetic resonance has quite good properties. Different from low power charging such as RF, magnetic resonance has high charging efficiency and can be easily realized by using copper coils with low costs. As shown in [2], when the distance is $1m$, the charging efficiency of magnetic resonance is 0.78, which is much higher than that of RF. The charging efficiency of magnetic resonance depends on the physical properties of coils. If the radii of the coils increase further, better charging efficiency can be obtained. This also makes multi-hop charging possible. Even after several hops, the charging efficiency is still considerable.

- *S. Wu, L. Xu, L. Liu, F. Xiao and J. Xu are with the Jiangsu Key Laboratory of Big Data Security and Intelligent Processing, Nanjing University of Posts and Telecommunications, Nanjing, Jiangsu 210023, China. (E-mail: 1019041115@njupt.edu.cn, ljxu@njupt.edu.cn, liulf@njupt.edu.cn, xiaof@njupt.edu.cn, xujia@njupt.edu.cn).*
- *H. Dai is with the State Key Laboratory for Novel Software Technology, Nanjing University, Nanjing, Jiangsu 210023 China. (E-mail: haipengdai@nju.edu.cn).*
- *Corresponding author: Jia Xu*

Manuscript received April 19, 2005; revised August 26, 2015.

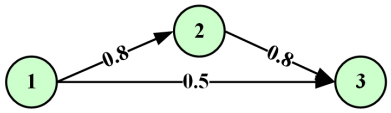

Fig. 1. Illustration of multi-hop wireless charging. The numbers on the edges represent the charging efficiency.

Multi-hop wireless charging [2, 9, 10] is a new charging model and is different from the traditional single-hop wireless charging [6-8, 11, 12]. In single-hop wireless charging, the sensor nodes only receive energy from the charger. While in multi-hop wireless charging, the sensor nodes not only receive energy from the charger, but also transfer energy to other sensor nodes.

Compared with single-hop wireless charging, multi-hop wireless charging has some promising advantages: (1) Multi-hop wireless charging can improve the charging efficiency [2]. The charging efficiency decreases dramatically with the charging distance no matter what charging technology is adopted. Multi-hop wireless can reduce the charging distance through adding the energy relays. As illustrated in Fig. 1, the charging efficiency from sensor node 1 to sensor node 3 is 0.5 if the energy is transferred directly. If the energy is transferred via sensor node 2, the charging efficiency is 0.8*0.8=0.64. Thus, the charging efficiency increases through multi-hop wireless charging. (2) In some situations, it is difficult to use single-hop wireless charging. For example, in the scenarios of building structure monitoring or disaster relief, the chargers cannot be placed in the desired positions due to the environmental limitation. Nevertheless, the energy can be transferred through multi-hop relays. (3) Multi-hop wireless charging is a flexible extension of single-hop wireless charging, and can provide better performance for

the optimization, such as cost minimization. In other words, single-hop wireless charging is a special case of multi-hop wireless charging. (4) In the case of mobile charging, multi-hop wireless charging can reduce the moving cost or the number of mobile chargers because the sensor nodes can relay the energy through multi-hop wireless charging.

A practical application of multi-hop wireless charging is called WiTricity [13], which develops the wireless charging technology based on magnetic resonance. To extend the wireless charging range, resonant repeaters are placed between the source and receiver, and are designed to allow power to hop over greater distances.

There have been some studies for optimizing multi-hop wireless charging [2, 14, 15]. These works optimize the single objective, such as the number of chargers, moving cost, or energy consumption. For example, Wang *et al.* [2] optimized the energy cost of multi-hop wireless charging in mobile charging scenario. Rault *et al.* [14] aimed to find the least chargers that can fulfill the energy demands of all sensor nodes. However, the single objective cannot represent the actual expenditure of wireless charging.

There are three modes of multi-hop wireless charging technology: store and forward, direct flow, and hybrid [9]. In store and forward mode, the sensor node accepts and stores energy first, and then forwards it to the sensor nodes of next hop. In direct flow mode, there is no storage in the midway, and the energy is directly sent to the target node via multiple hops. The hybrid mode is a mixture of the above two modes. In this paper, we consider the store and forward mode.

In this paper, we consider that the actual cost of wireless charging consists of energy cost and deployment cost. The energy cost is the expenditure for energy consumption (e.g., the payment to energy provider), and the deployment cost is the expenditure for deploying wireless chargers (e.g., rental fee, depreciation allowances, or installation cost), which depends on the number of deployed wireless chargers. We aim to optimize the comprehensive cost, which is the summation of energy cost and deployment cost, such that the energy demand of all sensor nodes can be fulfilled by energy capacitated chargers in the way of multi-hop energy transfer. Recall that the energy forwarding of every hop will lead to energy loss. Therefore, with the increasing number of hops, the energy loss increases accordingly. Deploying more chargers can help to reduce the overall energy consumption, but will increase the deployment cost.

A special problem of magnetic resonance that needs to be concerned is called "conflict" [2], that is, if multiple transmitters charge the same receiver simultaneously, the magnetic fields of the transmitters will affect each other. If they are not exactly in the same direction, there will be partial offset, resulting in energy loss. This "conflict" phenomenon degrades the charging efficiency and should be avoided. In fact, the concurrent magnetic resonance charging must work with conflict avoidance scheme. In Section 6, we propose the conflict avoidance schemes based on the asynchronous charging. Using the conflict avoidance scheme, "many-to-one" asynchronous charging can be realized theoretically. However, "many-to-one" asynchronous charging will cause huge communication cost to conflict avoidance scheme. More details will be presented in Section 6. Therefore, we aim to avoid "many-to-one" charging when we optimize the comprehensive cost. Note that "one-to-many" charging is feasible.

The problem of optimizing the comprehensive cost for charger deployment using magnetic resonance multi-hop wireless energy transfer in WRSN is very challenging. First, our problem is a variation of *Facility Location* problem. The chargers and the sensor nodes can be viewed as the facilities and clients, respectively. Thus, our problem can be viewed as opening a set of facilities such that the total cost of opening facilities and connecting clients to the facilities is minimized. However, the special of our problem is that the energy will flow to the sensor nodes via multiple hops. In order to avoid magnetic field interference, we need to assure that every sensor node along the energy flow is charged by the same charger. This makes the common solutions [16] of *Facility Location* problem invalid for our problem since it assumes that any client can be connected to any facility. Second, our problem also can be viewed as placing the chargers to cover all sensor nodes. The classic method to solve the covering problem is to assign the subset of sensor nodes to chargers greedily. Following this greedy method, we should decide on the subset of sensor nodes assigned to any charger. However, each charger has a limited energy capacity, and the solution needs to satisfy the energy constraints of deployed chargers.

The main contributions of this paper are as follows:

- We present a novel multi-hop wireless charging model and formulate the *Capacitated Comprehensive Cost Optimization* (C^3O) problem. To the best of our knowledge, we are the first to optimize the comprehensive cost and design the cost sharing mechanism for multi-hop wireless charging.
- We propose a $(\ln n + 1)$ -approximation algorithm for the C^3O problem, where n is the number of sensor nodes. We show that the designed algorithm can be extended to deal with the situation where the chargers can be placed anywhere.
- We propose a straightforward cost sharing mechanism, which can sustain cooperation among all sensor nodes served by the same charger in an economically stable manner. We show that the proposed cost sharing mechanism can satisfy the properties of local budget balance and local *core*.
- We propose the conflict avoidance schemes in both central and distributed situations through charging scheduling.
- Through extensive simulations, we demonstrate the significant superiority of the proposed algorithms in terms of comprehensive cost and strong adaptivity for parameter variations.

The rest of the paper is organized as follows. Section 2 presents a brief review on the previous works. Section 3 presents the system model and problem formulation. Section 4 presents the details of our solution. Section 5 presents the cost sharing mechanism. Section 6 presents the conflict avoidance schemes. We give the performance evaluation in Section 7. In Section 8, we discuss the distributed solution. We conclude this paper in Section 9.

2 Related Work

In this section, we briefly review the related work on single-hop wireless charging and multi-hop wireless charging.

2.1 Single-hop Wireless Charging

As the traditional charging mode, single-hop wireless charging has been widely studied. Dai *et al.* [6] studied the problem of charging task scheduling for directional wireless charger networks. They scheduled the orientations of chargers with time in centralized offline and distributed online fashions to maximize the overall charging utility for all tasks. Ma *et al.* [17] investigated the use of a mobile charger to charge multiple sensors simultaneously in WRSNs under the energy capacity constraint on the mobile charger. They aimed to minimize the sensor energy expiration time by formulating a novel charging utility maximization problem, where the amount of utility gain by charging a sensor was proportional to the amount of energy received by the sensor. In [18], a greedy algorithm is designed to find a recharge sequence that maximizes network lifetime using mobile chargers. In [19], an optimization problem is studied to maximize the ratio between charging vehicle's idling and working time. Although these articles solved their own goals, they did not consider the cost or just took the cost as a constraint instead of optimizing it.

Wang *et al.* [7] aimed to find the optimal trajectory planning for the mobile charger with objective of energy minimization. They designed an algorithm to find the trade-off between charging efficiency and trajectory distance. Zhou *et al.* [20] combined wireless charging technology with multi-source energy acquisition technology to build a self-sustainable network. They proposed a three-step solution to optimize this new framework. They first solved the Sensor Composition Problem (SCP) to derive the percentage of different types of sensors. Then they enabled self-sustainability by bringing energy harvesting storage to the field for charging the Mobile Charger (MC). Next, they proposed a 3-factor approximation algorithm to schedule sensor charging and energy replenishment of MC. Although they considered the cost of charger deployment, they did not consider the charging cost and traveling cost. In [21], the authors proposed a hybrid framework that combined the wireless charging with solar energy harvesting. They divided the network into three hierarchical levels and carried out the cost optimization in each level. However, the charging range of single-hop wireless charging is limited, thus, the moving cost of mobile charger is high. In [11], the authors presented a wireless charging service model from the perspective of cooperative charging economics, and formulated the Cooperative Charging Scheduling (CCS) problem for joint optimization of rechargeable devices' charging cost and moving cost. But the the number of chargers was determined in advance, which actually avoided considering the cost of this part.

2.2 Multi-hop Wireless Charging

There are some researches on charger deployment in multi-hop wireless charging. Rault *et al.* [14] aimed to place the chargers on sensor nodes. They proposed an optimization model of minimizing the number of chargers, which transferred energy to sensor nodes in the multi-hop wireless charging scenario. Wu *et al.* [15] proposed the repeater deployment method to realize full multi-hop wireless charging coverage of WRSN such that the number of resonant repeaters is minimized. They designed the rules to remove redundant repeaters and optimized the positions of necessary repeaters to improve the charging efficiency. However, neither [14] nor [15] took into consideration the energy cost.

In [2] and [22], the researchers considered the multi-hop wireless charging in a mobile charging scenario. With the multi-hop wireless charging technology, it is not necessary to visit all sensor nodes in the network. Wang *et al.* [2] carried out the regional partition through set cover algorithm, and then designed an algorithm to schedule the mobile chargers. Li *et al.* [22] proposed an energy efficient mobile multi-hop charging strategy. By introducing the optimal central point-based polling point selection algorithm, they constructed the best arrest point of each partition for the mobile charger. In each partition, the multi-hop wireless charging was adopted to replenish energy for these nodes. However, the distribution of charging areas will influence the energy consumption of mobile chargers. If the number of charging areas increases, more energy is needed in traveling. These papers also did not optimize the energy consumption and deployment cost jointly.

3 System Model and Problem Formulation

In this section, we present the system model and formulate the C^3O problem.

3.1 System Model

We consider that there is a WRSN consisting of a set $V = \{1, 2, ..., n\}$ of n sensor nodes, which can transfer energy to other sensor nodes. Each sensor node $j \in V$ has an energy demand $D_j \geq 0$. We denote the energy demand profile of all sensor nodes as $\mathbf{D} = (D_1, D_2, ..., D_n)$. The chargers are deployed at the positions of sensor nodes since the charger deployment can be viewed as installing high capacity battery to some sensor nodes. Thus, we reuse the notation V to represent the candidate positions of charger deployment. If the chargers may not be deployed on all sensor nodes, we simply remove the unviable positions from the candidate positions of charger deployment. We assume that the chargers are homogeneous, and each charger has the same energy capacity D_{MAX}, $D_{\mathrm{MAX}} \gg D_j$ for all $j \in V$. The sensor nodes also have the same energy capacity D_{MAX}. Note that the chargers can be deployed in any position of the whole square area, and the comprehensive cost can be reduced further. We will extend the C^3O problem by allowing the chargers to be deployed anywhere later.

If a sensor node does not receive energy from the prodromic sensor node, it cannot transfer energy to other sensor nodes. Even if the sensor node receives the energy, it will not forward the energy unless its energy demand is satisfied. If the distance between two sensor nodes exceeds the maximal charging range r, they cannot transfer energy to each other. We consider that all sensor nodes have same maximal charging range.

If the distance of any two sensor nodes $a, b \in V$ is within the maximal charging range r, we use π_{ab} to denote the

charging efficiency between them, $0 < \pi_{ab} \leq 1$. Based on [2], the charging efficiency is determined by the efficiency of both energy transmission and energy storage in the battery. Thus, the charging efficiency can stand for the practical losses of energy. According to [14], the charging efficiency is symmetrical, i.e., $\pi_{ab} = \pi_{ba}$ for any two sensor nodes $a, b \in V$. Specifically, $\pi_{ab} = 1$ iff $a = b$. The charging efficiency depends on the circuitry design of magnetic resonance, the distance between the two sensor nodes [3] and and the energy storage efficiency.

We define the charging network as follows:

Definition 1 (Charging Network). *The charging network is an undigraph $G(V, E)$, where V is the set of sensor nodes, E is the set of edges connecting the sensor nodes with distance less than the maximal charging range. Each edge $(a, b) \in E$ is with a charging efficiency $\pi_{ab} \in (0, 1]$.*

For any two sensor nodes $i, j \in V$, $(i, j) \notin E$, the initial charging efficiency between i and j is zero. However, if j obtains energy from i via a path P_{ij} from i to j on $G(V, E)$, the charging efficiency between i and j can be calculated as:

$$\pi_{ij} = \prod_{(a,b)\in E_{P_{ij}}} \pi_{ab} \tag{1}$$

where $E_{P_{ij}}$ is the set of edges in path P_{ij}.

Note that a sensor node cannot be charged by multiple chargers simultaneously due to the conflict of magnetic resonance wireless charging. Thus, if sensor node j is charged via path P_{ij} by charger i, then all sensor nodes in the path must be charged by charger i. This is because if any senor node on the path is charged by another charger, the senor node will not receive energy from charger i, and the sensor node must not belong to charging path P_{ij}. A paradox happens. In order to satisfy the energy demand of all nodes in path P_{ij}, the energy of charger i should be at least $\sum_{j'\in V_{P_{ij}}} \frac{D_{j'}}{\pi_{ij'}}$, where $V_{P_{ij}}$ is the set of sensor nodes in path P_{ij}. Any charger i can charge multiple sensor nodes via different paths. The paths with same source i together construct a charging tree.

Definition 2 (Charging Tree). *The charging tree is a subgraph of charging network $G(V, E)$. The charger locates in the root of charging tree, and the sensor nodes in charging tree (including the sensor node located in the root) are charged by the charger via the path of charging tree.*

We denote the charging tree with root $i \in V$ by T_i. The energy cost of charging tree T_i is $\alpha \sum_{j\in V_i} \frac{D_j}{\pi_{ij}}$, where α is the unit energy cost and V_i is the set of sensor nodes in T_i. Since a sensor node cannot be charged by multiple chargers, the deployment of chargers will divide the charging network into multiple disjoint charging trees, which construct a charging forest.

Definition 3 (Charging Forest). *The charging forest $\mathcal{T} = \{T_1, T_2, \ldots, T_k\}$ is a partition of charging network $G(V, E)$ by the disjoint charging trees, where k is the number of charging trees.*

Fig. 2 shows an example of the charging forest consisting of two disjoint charging trees. Here is an example of calculating the energy cost of the charging tree on the left. There are five sensor nodes in this tree, and the charger locates at the position of sensor node 1. The number beside the sensor nodes are their energy demand, i.e., $D_1 = D_2 = D_3 = 10$, $D_4 = 5$, $D_5 = 15$. The number on the edges represent the charging efficiency, i.e., $\pi_{11} = 1$, $\pi_{12} = \pi_{24} = 0.8$, $\pi_{15} = \pi_{23} = 0.5$. Based on Equation (1), we have $\pi_{13} = \pi_{12}\pi_{23} = 0.4, \pi_{14} = \pi_{12}\pi_{24} = 0.64$. Thus, the energy cost of charging tree T_1 is $\alpha \sum_{j\in V_1} \frac{D_j}{\pi_{1j}} = 85.3125\alpha$.

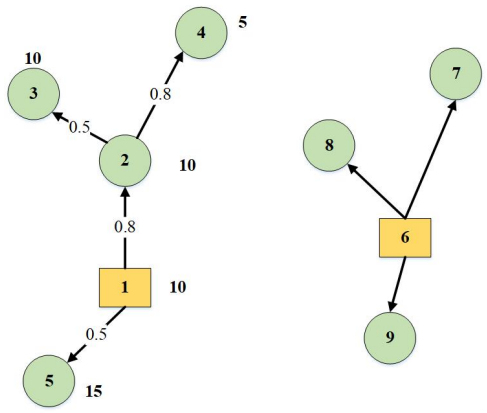

Fig. 2. Illustration of charging tree, charging forest, and energy cost.

Definition 4 (Comprehensive Cost). *The comprehensive cost F is the sum of energy cost and deployment cost:*

$$F{=}\alpha \sum_{i\in V} y_i \sum_{j\in V} \frac{D_j}{\pi_{ij}} x_{ij} + \beta \sum_{i\in V} y_i \tag{2}$$

where β is the deployment cost of a charger. $x_{ij} \in \{0, 1\}$ is the binary variable to indicate whether sensor node j is charged by charger i. $y_i \in \{0, 1\}$ is the binary variable to indicate whether a charger is placed at position i.

3.2 Problem Formulation

The objective is to construct the charging forest with capacitated energy of chargers such that the comprehensive cost is minimized. We refer to this problem as *Capacitated Comprehensive Cost Optimization* (C^3O) problem, which can be formulated as follows:

$$C^3O: \quad \min F{=}\alpha \sum_{i\in V} y_i \sum_{j\in V} \frac{D_j}{\pi_{ij}} x_{ij} + \beta \sum_{i\in V} y_i \tag{3}$$

$$s.t. \quad \sum_{i\in V} x_{ij} = 1, \ \forall j \in V \tag{3-1}$$

$$y_i \sum_{j\in V} \frac{D_j}{\pi_{ij}} x_{ij} \leq D_{\mathrm{MAX}}, \forall i \in V \tag{3-2}$$

$$x_{ij'} = 1, \ \ \forall j' \in V_{P_{ij}}, \ y_i = 1, x_{ij} = 1 \tag{3-3}$$

$$x_{ij} \in \{0, 1\}, \ \ \forall i, j \in V \tag{3-4}$$

$$y_i \in \{0, 1\}, \ \ \forall i \in V \tag{3-5}$$

The constraint (3-1) ensures that each sensor node is charged by exactly one charger. The constraint (3-2) ensures that the energy consumption of a charging tree is no more than the energy capacity of charger. The constraint (3-3) ensures that if a sensor node is charged by a charger, then all sensor nodes in the charging path from the charger to

the sensor node should be charged by the same charger. The constraints (3-4) and (3-5) state that x_{ij} and y_j are binary variables.

We list the frequently used notations in Table. I.

TABLE 1
Frequently Used Notations

Symbol	Description
$V,\ n$	Set of sensor nodes, Number of sensor nodes
D_j	Energy demand of sensor node j
D	Energy demand profile
r	Maximal charging range
π_{ij}	Charging efficiency between i and j
D_{MAX}	Energy capacity of charger
D_r	Residual energy of charger
$\alpha,\ \beta$	Unit energy cost, Unit deployment cost of charger
$G(V,E)$	Charging network
$\mathcal{T},\ T_i$	Charging forest, Charging tree with root i
$V_i,\ E_i$	Set of sensor nodes of T_i, Set of edges of T_i
P_{ij}	Charging path from i to j
$V_{P_{ij}}$	Set of sensor nodes in path P_{ij}
V_u	Set of uncovered sensor nodes
V_c	Possible positions of charger deployment
$F(T_i)$	Comprehensive cost of charging tree T_i
m	Number of newly covered sensor nodes
s	Number of rows and columns of regional discretization
$T_i(m)$	Charging tree after the m-th sensor node is added to T_i
$V_i(m)$	Set of sensor nodes in $T_i(m)$
$E_i(m)$	Set of edges in $T_i(m)$
$T^*{}_i$	Optimal capacitated extension tree of T_i
θ	Maximal communication distance
$cost_i\ (j)$	Average marginal comprehensive cost of $T^*{}_i$ when $T^*{}_i$ covers j

4 Algorithm Design for C^3O Problem

4.1 Hardness and Design Rationale

We give the hardness of C^3O in the following theorem.

Theorem 1. *The C^3O problem is NP-hard.*

Proof: We consider the special case of C^3O problem by removing the constraint (3-3). We first demonstrate that the special case of C^3O belongs to NP. Given an instance of the special case of C^3O, we can check whether the energy demand of all sensor nodes is fulfilled and whether the comprehensive cost is at most v. This process can terminate in polynomial time.

Next, we prove the NP-hardness of the special case of C^3O problem by giving a polynomial time reduction from the *Single Source Capacitated Facility Location* (*SSCFL*) problem, which is a well-known NP-hard problem [16].

Instance of *SSCFL* (denoted by *A*): For a set $L = \{1, 2, \cdots, n\}$ of n positions. Each position has a client and a facility. Let V be the client set. Each client $j \in V$ has a demand D_j that should be served by one open facility. The cost for serving one-unit demand of client j from facility i is α/π_{ij}. Let β denote the cost of opening a facility. Let D_{MAX} denote the maximum demand a facility can serve. The question is whether there exists a subset of open facilities such that the demand of each client can be satisfied by an open facility, and the total cost of facility opening and client service is at most v.

We consider a corresponding instance of the special case of C^3O problem (denoted by *B*): For a set $L = \{1, 2, \cdots, n\}$ of n positions, each position has a sensor node. The candidate positions for charger deployment is V. Each sensor node $j \in V$ has an energy demand D_j that should be charged by one charger. Let α denote the unit energy cost. Let π_{ij} denote charging efficiency for charging sensor node j from charger i. Therefore, the cost for charging one-unit energy of sensor node j from charger i is α/π_{ij}. Let β denote the deployment cost of a charger. Let D_{MAX} energy a charger can provide. The question is whether there exists a subset of positions for charger deployment such that the energy demand of each sensor node is fulfilled by a charger, and the total deployment cost and energy cost is at most v.

This reduction from *A* to *B* ends in polynomial time. We can simply see that q is a solution to *A* if and only if q is a solution to *B*. ■

Since the C^3O problem is NP-hard, it is impossible to obtain the optimal solution in polynomial time unless P=NP. In addition, the off-the-shelf algorithms [23, 24] for *SSCFL* problem cannot be used to solve C^3O problem since we need to guarantee that the solution outputs the disjoint charging trees.

On the other hand, the C^3O problem is equivalent to constructing a charging forest to cover all sensor nodes under the constraint of energy capacity such that the total comprehensive cost of all charging trees is minimized. We refer to this problem as P1, which can be formulated as:

$$\mathrm{P1}: \quad \min \sum_{T_i \in \mathcal{T}} F(T_i) \tag{4}$$

$$s.t. \quad V = \bigcup_{T_i \in \mathcal{T}} V_i \tag{4-1}$$

$$V_i \cap V_{i'} = \emptyset, \ \ \forall i \neq i',\ T_i \in \mathcal{T},\ T_{i'} \in \mathcal{T} \tag{4-2}$$

$$\sum_{j \in V_i} \frac{D_j}{\pi_{ij}} \leq D_{\mathrm{MAX}}, \ \ \forall T_i \in \mathcal{T} \tag{4-3}$$

where $F(T_i)$ is the comprehensive cost of charging tree T_i, which can be calculated as follows:

$$F(T_i) = \begin{cases} \alpha \sum\limits_{j \in V_i} \frac{D_j}{\pi_{ij}} + \beta, & V_i \neq \emptyset \\ 0, & V_i = \emptyset \end{cases} \tag{5}$$

The constraint (4-1) ensures that all sensor nodes can be covered by the charging forest. The constraint (4-2) ensures that all charging trees in the forest are disjoint. The constraint (4-3) ensures that the energy consumption of each charging tree is no more than the energy capacity of charger.

To solve P1, we consider that there is an empty charging tree at each position in V initially, then we extend these empty charging trees greedily until all sensor nodes are covered by the charging forest. In each extension, we tend to cover more sensor nodes with minimum marginal comprehensive cost, i.e., finding the extended charging tree with minimum average marginal comprehensive cost under energy capacity. Consider that we put some uncovered sensor nodes into a charging tree T_i (can be empty), and the extended charging tree is $T'{}_i$, then the average marginal comprehensive cost of extending T_i to $T'{}_i$ can be calculated as follows:

$$\frac{F(T'{}_i) - F(T_i)}{|V'{}_i \backslash V_i|} \tag{6}$$

i.e., the ratio of the marginal comprehensive cost to the number of newly covered sensor nodes.

Next, we define the optimal capacitated extension tree.

Definition 5 (Optimal Capacitated Extension Tree, OCET). *Given any charging tree T_i and the uncovered sensor node set V_u, the extended charging tree ${T^*}_i$ is the OCET of T_i if and only if its average marginal comprehensive cost is minimized under the constraint of energy capacity, i.e.,*

$$ {T^*}_i = \arg \min_{T'_i : V'_i \supset V_i, V'_i \backslash V_i \subseteq V_u} \frac{F(T'_i) - F(T_i)}{|V'_i \backslash V_i|} \quad (7) $$
$$ s.t. \quad \sum_{j \in V'_i} \frac{D_j}{\pi_{ij}} \leq D_{\mathrm{MAX}} $$

Obviously, to follow the greedy method, we need to determine the *OCET* for each T_i in each iteration. However, T_i can be extended by adding any subset of uncovered sensor node set V_u. It will take exponential time to enumerate all possible subset of V_u.

To address this issue, we present an enhanced Prim algorithm to extend each T_i. At each time, the uncovered sensor node with minimum energy consumption is merged to T_i. We record every extended charging tree once a sensor node is merged. Finally, the enhanced Prim algorithm will find a minimum spanning tree under the constraint of energy capacity. Then, we find the extended charging tree with minimum average marginal comprehensive cost among all recorded extended charging trees. We will show that this extended charging tree is *OCET* of T_i. The above process can be finished in polynomial time.

4.2 Algorithm Design

In this section, we propose the approximation algorithm, termed *Capacitated Comprehensive Cost Optimization Algorithm* (C^3OA) to solve C^3O problem.

As illustrated in Algorithm 1, we set an empty charging tree for every position in V(Line 1). Then we try to extend these charging trees to cover all sensor nodes. Let V_u and V_c be the set of uncovered sensor nodes and the set of possible positions of charger deployment, respectively. We set $V_u = V_c = V$ initially (Line 2).

For each possible position of charger deployment $i \in V_c$, we find the *OCET* of T_i by calling function $EnPrim(\cdot)$ (Line 5). Note that the charging tree returned by $EnPrim(\cdot)$ is an extended charging tree from either a nonempty charging tree or an empty charging tree.

Then we find the charging tree ${T^*}_i$ with the minimum average marginal comprehensive cost among all *OCETs* (Line 7). The charging tree T_i is extended to ${T^*}_i$ (Line 8). Finally, we update the set V_u and V_c (Line 8). Note that the set V_c should contain the positions of all uncovered sensor nodes and all deployed chargers, i.e., V_c=$V_c \backslash (V_i \backslash \{i\})$.

The iteration terminates when all sensor nodes are covered, i.e., $V_u = \emptyset$ (Line 3).

The function $EnPrim(\cdot)$ illustrated in Algorithm 2 returns the *OCET*. Given the charging tree T_i, let m be the number of newly covered sensor nodes. Let $T_i(m)$ be the charging tree after the m-th sensor node is added to T_i. Let $V_i(m)$ and $E_i(m)$ are the set of sensor nodes and set of edges of $T_i(m)$, respectively. Let ${V'}_u$ be the uncovered sensor nodes in the process of tree extension. Let D_r be the residual energy of charger i. The parameter initialization is given in Line 1.

If the inputting charging tree T_i is empty, the sensor node i is added to T_i first (Line 2-4). Note that the energy capacity can always satisfy the energy demand of sensor node at position i since $D_{\mathrm{MAX}} \gg D_i$ for all $i \in V$.

The following process is constructing a minimum spanning tree under the constraint of energy capacity (Line 5-11). This can be realized by enhancing the well-known Prim algorithm. Specifically, we find the sensor node pair (j_i, j_o) with minimum energy consumption $\frac{D_{j_o}}{\pi_{ij_i}\pi_{j_ij_o}}$, where j_i is a sensor node in the charging tree $T_i(m)$. j_o is a sensor node outside $T_i(m)$. $\pi_{ij_i}\pi_{j_ij_o} = \pi_{ij_o}$ is the charging efficiency from charger i to sensor node j_o (Line 6). If the residual energy of charger i can satisfy the energy demand of sensor node j_o, we increase the number of newly covered sensor nodes, and the sensor node j_o is added to $T_i(m)$ (Line 7-8). If the residual energy of charger i cannot satisfy the energy

Algorithm 1 : C^3OA

Input: charging network $G(V, E)$, energy capacity D_{MAX}, energy demand profile $\mathbf{D}$

1: **foreach** $i \in V$ **do** $T_i = (V_i, E_i) \leftarrow (\emptyset, \emptyset)$;
2: $V_u \leftarrow V$; $V_c \leftarrow V$; $\mathcal{T} \leftarrow \{T_1, T_2, \ldots, T_n\}$;
3: **while** $V_u \neq \emptyset$ **do**
4: **foreach** $i \in V_c$ **do**
5: ${T^*}_i \leftarrow EnPrim(T_i, V_u, G(V, E), D_{\mathrm{MAX}}, \mathbf{D})$;
6: **end**
7: $i \leftarrow \arg \min_{i' \in V_c, {V^*}_{i'} \backslash V_{i'} \neq \emptyset} \frac{F({T^*}_{i'}) - F(T_{i'})}{|{V^*}_{i'} \backslash V_{i'}|}$;
8: $T_i \leftarrow {T^*}_i$; $V_u \leftarrow V_u \backslash V_i$; $V_c \leftarrow V_c \backslash (V_i \backslash \{i\})$;
9: **end**
10: **return** $\mathcal{T}$;

Algorithm 2 : $EnPrim$

Input: charging network $G(V, E)$, energy capacity D_{MAX}, energy demand profile $\mathbf{D}$, charger tree T_i, set of uncovered sensor nodes V_u

1: $m \leftarrow 0$; $m_{\mathrm{MIN}} \leftarrow 0$; $V_i(m) \leftarrow V_i$; $E_i(m) \leftarrow E_i$; ${V'}_u \leftarrow V_u$; $D_r \leftarrow D_{\mathrm{MAX}} - \sum_{j \in V_i} \frac{D_j}{\pi_{ij}}$;
2: **if** $V_i = \emptyset$ **then**
3: $m \leftarrow m + 1$; $V_i(m) \leftarrow V_i(m-1) \cup \{i\}$; $D_r \leftarrow D_r - D_i$; ${V'}_u \leftarrow {V'}_u \backslash \{i\}$;
4: **end**
5: **while** $D_r > 0$ **do**
6: $(j_i, j_o) \leftarrow \arg \min_{(j,j') \in E_i(m): j \in V_i(m), j' \in {V'}_u} \frac{D_{j'}}{\pi_{ij}\pi_{jj'}}$;
7: **if** $D_r - \frac{D_{j_0}}{\pi_{ij_i}\pi_{j_ij_o}} \geq 0$ **then**
8: $m \leftarrow m + 1$; $D_r \leftarrow D_r - \frac{D_{j_0}}{\pi_{ij_i}\pi_{j_ij_o}}$; $\pi_{ij_o} \leftarrow \pi_{ij_i}\pi_{j_ij_o}$; ${V'}_u \leftarrow {V'}_u \backslash \{j_o\}$; $V_i(m) \leftarrow V_i(m-1) \cup \{j_o\}$; $E_i(m) \leftarrow E_i(m-1) \cup \{(j_i, j_o)\}$;
9: **else break;**
10: **end**
11: **end**
12: $m_{\mathrm{MIN}} \leftarrow \arg \min_{m' > 0} \frac{F(T_i(m')) - F(T_i)}{m'}$;
13: **return** $T_i(m_{\mathrm{MIN}})$;

demand of sensor node j_o, we can conclude that no sensor node can be added to $T_i(m)$ since j_o is the sensor node with the minimum energy consumption among all uncovered sensor nodes, and the minimum spanning tree construction terminates (Line 9).

Finally, we find the extended charging tree $T_i(m_{\text{MIN}})$ with the minimum average marginal comprehensive cost among all extended charging trees (Line 12), where m_{MIN} is the index of *OCET*.

4.3 Algorithm Analysis

Theorem 2. *EnPrim returns the OCET of any given charging tree T_i.*

Proof: Given any charging tree T_i, Let m_{MAX} indicate the maximum number of added sensor nodes under the energy capacity constraint. Let m_{PRIM} indicate the number of added sensor nodes using *EnPrim* under the energy capacity constraint. Since *EnPrim* adds the sensor node with the minimum energy consumption, the number of added sensor nodes can be maximized, i.e., we have m_{MAX}=m_{PRIM}. Thus, $EnPrim$ can enumerate all possible values of $m \in 1, 2, ..., m_{\text{MAX}}$.

Given any $m \in \{1, 2, ..., m_{\text{MAX}}\}$ and charging tree T_i, *EnPrim* can return the minimum spanning tree when exactly m sensor nodes are added through Prim algorithm, where the cost of any sensor node j is $\frac{D_j}{\pi_{ij}}$. Note that the Prim algorithm begins with a nonempty tree since the root of the tree is fixed, thus the deployment cost should not be involved in the cost of sensor node. Thus, $T_i(m)$ is a tree minimizing $\sum_{j \in V_i(m)} \frac{D_j}{\pi_{ij}}$ for fixed m. We have the following equivalence transformations:

$$\begin{aligned}
&\min \sum_{j \in V_i(m)} \frac{D_j}{\pi_{ij}} \\
&\Leftrightarrow \min \frac{\sum_{j \in V_i(m)} \frac{D_j}{\pi_{ij}}}{m} \\
&\Leftrightarrow \min \frac{\sum_{j \in V_i(m)} \frac{D_j}{\pi_{ij}} - \sum_{j \in V_i} \frac{D_j}{\pi_{ij}}}{m}
\end{aligned} \tag{8}$$

$$\begin{aligned}
&\Leftrightarrow \min \frac{(\alpha \sum_{j \in V_i(m)} \frac{D_j}{\pi_{ij}} + \beta) - (\alpha \sum_{j \in V_i} \frac{D_j}{\pi_{ij}} + \beta)}{m} \\
&\Leftrightarrow \min \frac{F(T_i(m)) - F(T_i)}{m}
\end{aligned}$$

The first equivalence relies on that m is a fixed number. The second equivalence is because T_i is a given charging tree, and the value of $\sum_{j \in V_i} \frac{D_j}{\pi_{ij}}$ is a constant. The last equivalence is based on the definition of comprehensive cost of any charging tree, which is given in Equation (5).

Since *EnPrim* enumerates all possible values of m under the energy capacity constraint and find m_{MIN} as the optimal m such that $\frac{F(T_i(m))-F(T_i)}{m}$ is minimized, we can conclude $T_i(m_{\text{MIN}}) = {T^*}_i$ based on Equation (7):

$$\begin{aligned}
T_i(m_{\text{MIN}}) &= \arg \min_{T_i(m): m \in \{1,2,...,m_{\text{MAX}}\}} \frac{F(T_i(m))-F(T_i)}{m} \\
&= \arg \min_{T'_i: V'_i \supset V_i, V'_i \setminus V_i \subseteq V_u} \frac{F(T'_i)-F(T_i)}{|V'_i \setminus V_i|} \\
&= {T^*}_i
\end{aligned} \tag{9}$$

where ${T^*}_i$ is the *OCET* of charging tree T_i. ■

Theorem 3. *The time complexity of C^3OA is $O(n^5)$.*

Proof: The running time of C^3OA is dominated by the function $EnPrim(\cdot)$ (Line 5 of Algorithm 1). The while-loop (Line 3-9 of Algorithm 1) takes $O(n)$ since each iteration will cover at least one sensor node. The for-loop (Line 4-6 of Algorithm 1) takes $O(n)$ since there are at most n possible positions of charger deployment. The running time of *EnPrim* (Algorithm 2) is dominated by finding the sensor node pair (j_i, j_o) with minimum energy consumption (Line 6 of Algorithm 2), which takes $O(n^2)$ time. Since there are at most $n-1$ sensor nodes outside the changing tree, the running time of *EnPrim* is $O(n^3)$. Thus, the running time of C^3OA is $O(n^5)$. ■

Theorem 4. *C^3OA is a $(\ln n + 1)$-approximation algorithm of the C^3O problem.*

Proof: Number the sensor nodes of V in the order in which they were covered by C^3OA, resolving ties arbitrarily. Let $j_1, j_2, ..., j_n$ be this numbering. Assume $j_k, k = 1, 2, ..., n$ is covered by *OCET* ${T^*}_i$ of T_i, we define the comprehensive cost effectiveness of j_k as

$$cost(j_k) = \frac{F({T^*}_i) - F(T_i)}{|{V^*}_i \setminus V_i|} \tag{10}$$

Let OPT be the optimal comprehensive cost of P1. Consider the iteration in which j_k was covered, the charging forest of the optimal solution can cover the remaining sensor nodes in V_u at a comprehensive cost of at most OPT. Therefore, among all charging trees in the optimal charging forest, there must be one having comprehensive cost effectiveness at most $OPT/|V_c|$, where $|V_c| \geq n-k+1$. Since j_k was covered by ${T^*}_i$ with minimum comprehensive cost effectiveness in this iteration, it follows that

$$cost(j_k) \leq \frac{OPT}{|V_c|} \leq \frac{OPT}{n-k+1} \tag{11}$$

Since the comprehensive cost of each charging tree is distributed among the new sensor nodes covered, the total comprehensive cost of the charging forest obtained by C^3OA is equal to $\sum_{k=1}^{n} cost(j_k) \leq \sum_{k=1}^{n} \frac{OPT}{n-k+1} = (1 + \frac{1}{2} + ... + \frac{1}{n})OPT \leq (\ln n + 1)OPT$

Since P1 is equivalent to C^3O problem, C^3OA is a $(\ln n + 1)$-approximation algorithm of the C^3O problem. ■

Remark: Any tie breaking rule can be adopted for Line 7 in Algorithm 1, Line 6 in Algorithm 2, and Line 12 in Algorithm 2, and the stated approximation ratio still holds.

4.4 Extended C^3OA

In this subsection, we analyze the practical scenario that chargers can be deployed anywhere, and propose a heuristic algorithm based on the idea of C^3OA.

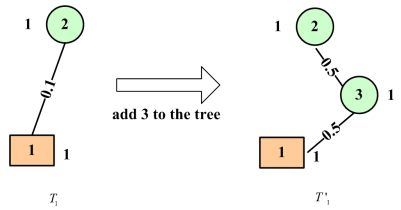

Fig. 3. An example to illustrate that *Shapley Value* method is inapplicable. The numbers beside the sensor nodes are energy demand. The numbers on the edges represent the charging efficiency.

If the chargers can be deployed in any positions of whole region, further improvement of comprehensive cost can be achieved. However, the possible deployment positions are infinite. A widely adopted method is region discretization [25], which divides the whole region into multiple sub regions, and the positions in the same sub region are viewed as the identical position approximatively with a small error. However, in our problem, due to the energy capacity of chargers, if there is an error in the calculation of energy cost, the shapes of charging trees and the number of chargers will change. Therefore, it is difficult to obtain the performance gap from the optimal solution.

We proposed a heuristic algorithm based on the idea of C^3OA. First, we divide the whole region into $s \times s$ sub regions and remove the unviable sub regions where the chargers cannot be deployed. Each residual sub region can be viewed as a candidate charger deployment position. Then, we can execute C^3OA for all candidate charger deployment positions to solve the extended C^3O problem, and the running time is $O(s^2n^4)$ according to Theorem 3. We term the extended C^3OA as EC^3OA.

5 Cost Sharing Mechanism

In this section, we consider the problem of cost sharing in multi-hop wireless charging. In section 4, we have determined the charging forest, which can be viewed as a set of coalitions of sensor nodes for cooperative charging. Since we consider that the comprehensive cost is the actual expenditure for wireless charging, we need a cost sharing mechanism to share the comprehensive cost (sometimes called cost-sharing game).

The concept of *core* [26], which sustains cooperation among all users in an economically stable manner, is an important property in cost sharing mechanism design. The *core* property requires to calculate the comprehensive cost of any possible subsets of sensor nodes. However, we state that there is no nonempty *core* for our multi-hop wireless charging. This is because there may be multiple feasible charging trees even both the charger position and the subset of sensor nodes are fixed. Thus, the comprehensive cost of any fixed charger position and subset of sensor nodes is not unique. The uncertainty makes the economically stable cooperation of sensor nodes impossible.

If the *core* of a cost-sharing game is empty, the classic *Shapley Value* method [27], which charges each user the marginal cost of adding it to the serviced set, is widely used to share the total cost to the users fairly. However, the marginal cost may be negative in our game. We give an example illustrated in Fig. 3 to show that the classic *Shapley Value* method is also inapplicable. The charging tree T_1 has two sensor nodes in the beginning, and the charger locates at position 1. $D_1 = D_2 = 1$, $\pi_{11} = 1$, $\pi_{12} = 0.1$. According to Equation (5), the comprehensive cost of T_1 is $F(T_1) = \alpha(\frac{D_1}{\pi_{11}} + \frac{D_2}{\pi_{12}}) + \beta = 11\alpha + \beta$. Now we add sensor node 3 into the subset, and one of the possible charging trees is T'_1, where $D_3 = 1$, $\pi_{13} = \pi_{23} = 0.5$. We have $F(T_1) = \alpha(\frac{D_1}{\pi_{11}} + \frac{D_3}{\pi_{13}} + \frac{D_2}{\pi_{13}\pi_{23}}) + \beta = 7\alpha + \beta$. Thus, the marginal cost of sensor node 3 is -4α.

Since the *core* is empty and the *Shapley Value* method is inapplicable. It is hopeless to design a global cost sharing mechanism. To address this problem, we propose a straightforward cost sharing mechanism for local charging tree, i.e., the cost sharing mechanism for the sensor nodes in each given charging tree. For given charging tree T_i, the cost share of any sensor node $j \in V_i$ is:

$$F_j(T_i) = \alpha\frac{D_j}{\pi_{ij}} + \frac{\beta}{|V_i|} \tag{12}$$

i.e., the cost share of any sensor node $j \in V_i$ is the sum of its energy cost and the average deployment cost.

Despite its simplicity, we show that the designed cost sharing mechanism can achieve some desirable properties.

Definition 6 (Local Budget Balance). *Given the fixed position of charger $i \in V$ and the corresponding charging tree T_i, the cost sharing mechanism satisfies the property of local budget balance if* $\sum_{j\in V_i} F_j(T_i) = F(T_i)$.

Definition 7 (Local Core). *Given the fixed position of charger $i \in V$ and the corresponding subset V_i of sensor nodes, the cost sharing mechanism satisfies the property of local* core *if* $\sum_{j\in V'_i} F_j(T_i) \le F(T'_i)$ *for any* $V'_i \subseteq V_i$.

The property of local budget balance ensures that the summation of the individual cost share equal to the comprehensive cost for any charging tree. The property of local *core* ensures that no subset of sensor nodes can benefit by breaking away from the current charging tree for any fixed charger position.

Theorem 5. *The cost sharing mechanism satisfies the properties of local budget balance and local* core.

Proof: Obviously, our cost sharing mechanism satisfies the property of local budget balance. To prove the property of local *core*, we consider the following two situations:

(1) $T'_i \subseteq T_i$, i.e., T'_i is a subtree of T_i.

For any $j \in V'_i$, we have

$$\sum_{j\in V'_i} F_j(T_i) = \sum_{j\in V'_i} (\alpha\frac{D_j}{\pi_{ij}} + \frac{\beta}{|V_i|}) = \sum_{j\in V'_i} \alpha\frac{D_j}{\pi_{ij}} + \frac{\beta|V'_i|}{|V_i|}$$
$$\le \sum_{j\in V'_i} \alpha\frac{D_j}{\pi_{ij}} + \beta = F(T'_i)$$

(2) $T'_i \not\subset T_i$, i.e., some intermediate nodes are removed from T_i.

In this case, for any $j \in V'_i$, the charging efficiency between sensor node j and charger i may be different in T_i and T'_i. We denote the charging efficiency between sensor node j and charger i in T_i and T'_i as π_{ij} and π'_{ij}, respectively. Note that we are sharing the cost of charging tree T_i obtained by C^3OA. Since C^3OA always outputs the charging tree with minimum energy cost, we have $\pi'_{ij} \le \pi_{ij}$. For any $j \in V'_i$, we have

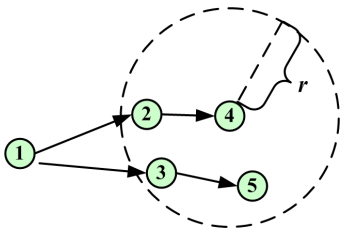

Fig. 4. Illustration of conflict.

$$\sum_{j\in V'_i} F_j(T_i) = \sum_{j\in V'_i} (\alpha\frac{D_j}{\pi_{ij}} + \frac{\beta}{|V_i|}) = \sum_{j\in V'_i} \alpha\frac{D_j}{\pi_{ij}} + \frac{\beta|V'_i|}{|V_i|}$$
$$\leq \sum_{j\in V'_i} \alpha\frac{D_j}{\pi'_{ij}} + \beta = F(T'_i)$$

Overall, the properties of local budget balance and local *core* can be satisfied. ■

6 Conflict Avoidance Scheme

In Section 4, we have constructed the charging forest to ensure that a receiver only obtain energy from one transmitter. However, in the actual implementation, the conflict may happen when multiple adjacent transmitters work simultaneously. For the example illustrated in Fig. 4, there is a subtree, where the arrows represent the energy flows. We consider both sensor node 2 and sensor node 3 are in the charging range of sensor node 4. If sensor node 2 and sensor node 3 transmit energy simultaneously, the magnetic field of sensor node 2 will be affect by the magnetic field of sensor node 3 at the position 4. The conflict happens.

To address this issue, we need the conflict avoidance scheme. In this section, we propose a central conflict avoidance scheme and a distributed conflict avoidance scheme to avoid the conflict.

6.1 Central Conflict Avoidance Scheme

For convenience, we termed the non-leaf nodes in the charging forest as transmitters. Since each transmitter needs to discharge exactly once, we can avoid the conflict by a well-designed schedule for the discharging tasks of all transmitters.

We employ a central server to schedule the discharging tasks. The basic idea is to maintain a conflict graph for the transmitters which are ready to perform the discharge tasks, and use the classic graph coloring algorithm [28] to select a set of transmitters with same color to perform the discharge tasks at each time.

First, we give the concept of conflict set.

Definition 8 (Conflict Set). *The conflict set of any transmitter is a set of other transmitters, which is in the maximum charging range of any child of the transmitter.*

To implement our conflict avoidance scheme, we define two sets: working transmitter set and candidate transmitter set. We schedule the discharging tasks as follows:

Step 1: Initially, we put all transmitters into the candidate transmitter sets. We set working transmitter set as empty.

Step 2: We select the transmitters, which satisfy the following two conditions, in the candidate transmitter sets: (1) the transmitter is ready to perform the discharging task (the energy demand of itself has been fulfilled); (2) The transmitters in its conflict set are not in the working transmitter set.

Step 3: We construct a conflict graph for the transmitters selected by Step 2. For each transmitter, we add conflict edges connecting to other selected transmitters in its conflict set.

Step 4: We use the classic graph coloring algorithm, and select a set of transmitters with same color to perform the discharge tasks immediately. We move these transmitters from the candidate transmitter set to the working transmitter set. Let the transmitters in the working transmitter set start transmitting energy.

Step 5: If the energy demand of a sensor node is met, a acknowledgment message is returned to the central server. When all sensor nodes in the charging tree returned the acknowledgment messages, the charging task of the transmitter is completed, and we remove the transmitter from the working transmitter set, and add its downstream transmitters into the candidate transmitter set.

Step 6: repeat Step 2 to Step 5 until the candidate transmitter set becomes empty.

Remark: Any set of transmitters with same color can be selected in Step 4. Many criterions, such as selecting the transmitter set with most children in the charging forest, selecting the transmitter set with most energy demand of their children, can be applied for color selection.

6.2 Distributed Conflict Avoidance Scheme

In the distributed scenario, the central scheduling of the discharging tasks is impossible. We employ the classic CSMA/CD [29] as the conflict detection protocol. Since the maximum communication range of the sensor nodes is much larger than the maximum charging range, the conflict set of any transmitter can be obtained by locally exchanging the location information with its neighbors. If a transmitter wants to discharge, it detects the working states of transmitters in its conflict set. If no transmitter in its conflict set is performing the discharging task, it starts discharging. Otherwise, it keeps detecting. If a transmitter has detected a conflict when it is discharging. The Binary Exponential Backoff Policy [30] is applied to determine the waiting time before the next detection. The process continues until the transmitter completes the discharging task.

6.3 Communication Cost

Although the proposed conflict avoidance Schemes can avoid conflicts, it is obvious that these methods will bring communication cost. Take the central conflict avoidance scheme as an example, if any sensor node is only charged by one transmitter, each sensor node needs to return one acknowledgment message only when its energy demand is fulfilled. Thus the number of acknowledgment messages (communication cost) is $O(n)$. On the other hand, a sensor node may obtain energy from multiple transmitters asynchronously (n transmitters in the extreme case) if "many-to-one" asynchronous charging is allowed, and each sensor node needs to at most n acknowledgment messages. Therefore, the total communication cost is $O(n^2)$ for whole

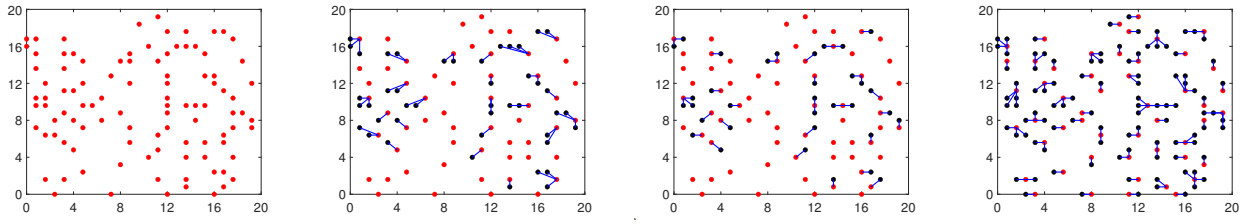

Fig. 5. Charger deployment. The red points represent the positions of chargers. The black points represent the positions without chargers. The sensor nodes of charging trees are connected by blue lines. (a) Minimum Energy. (b) Fewest Chargers for $\mathbf{C^3O}$. (c) $\mathbf{C^3OA}$. (d) $\mathbf{EC^3OA}$.

WRSN. Since message transmission is energy-intensive for sensor nodes, we do not consider the "many-to-one" asynchronous charging in this study.

7 Performance Evaluation

In this section, we conduct simulations to evaluate the performance of our proposed algorithms.

7.1 Simulation Setup

We compare our solution C^3OA with following two benchmark algorithms:

- *Minimum Energy*: Since the energy loss is negligible when the charger and the sensor node are located in the same position, *Minimum energy* deploys a charger in each position of sensor nodes to minimize the total energy consumption, which is the summation of energy demands of all sensor nodes actually.
- *Fewest Chargers for* C^3O [2]: We modify the charger selection algorithm in [2] by setting the efficiency threshold $\tau = 0$ and adding the energy capacity constraint such that the algorithm can deal with our system model. *Fewest Chargers for* C^3O selects the charging tree with the most sensor nodes greedily using energy constrained Prim algorithm to minimize the number of chargers approximately.

For the simulations, we uniformly distribute sensor nodes in a $20m \times 20m$ square area to simulate the dense *WRSN* environment of precision agriculture. We deploy various sensors, such as temperature sensors, humidity sensors, PH sensors, in a 400 square meter piece of farmland to accurately detect the condition of the piece of farmland. We set $n = 100$, $r = 2m$, $D_{\mathrm{MAX}} = 50KJ$, $\alpha = 0.25$, $\beta = 2.5$, $s = 25$ as the default setting. In our simulations, one unit of energy is $1KJ$, and the energy demand of each sensor node is randomly selected in $[0.8KJ,\ 1.2KJ]$. For any sensor nodes $a, b \in V$, the charging efficiency is calculated based on [3]:

$$\pi_{ab} = \begin{cases} 1, & a = b \\ \frac{Q_a Q_b \gamma}{16(d_{ab}/\sqrt{l_a l_b})^6}, & d_{ab} \le r,\ a \neq b \\ 0, & d_{ab} > r,\ a \neq b \end{cases} \tag{13}$$

where Q_a and Q_b are the quality factors of two resonators. γ is the energy storage efficiency. l_a and l_b are the radii of coils. d_{ab} is the distance between a and b. For our simulation, we set all quality factors as 1200 and all coil radii as 0.12 m, and set $\gamma = 25/36$, although our algorithm does not impose the assumption of homogeneous sensor nodes. Moreover, we consider $d_{ab} >> l_a$ and $d_{ab} >> l_b$ to guarantee $\pi_{ab} \le 1$.

We will vary the values of the key parameters to explore the impacts on designed algorithm. All the simulations are run on a Windows machine with Intel(R) Core(TM) i5-8300H CPU and 8 GB memory. Each measurement is averaged over 100 instances.

7.2 Charger Deployment

We first show the charger deployment for 100 sensor nodes of all algorithms in $20m \times 20m$ square area. Fig. 5(a), Fig. 5(b) , Fig. 5(c), and Fig. 5(d) depict the outputs of *Minimum Energy*, *Fewest Chargers for* C^3O, C^3OA, and EC^3OA, respectively. We can see that *Minimum Energy* deploys the charger for each position of sensor nodes. *Fewest Chargers for* C^3O constructs a total of 56 charging trees. C^3OA constructs a total of 66 charging trees. EC^3OA constructs a total of 51 charging trees.

7.3 Impact of Number of Sensor Nodes

Then we change the number of sensor nodes from 35 to 160, and measure the number of chargers, energy consumption, and comprehensive cost of all algorithms. We can see from Fig. 6(a) that the number of chargers of all algorithms increases. This is because the energy demand increases, and more chargers are needed to satisfy the energy demands of all sensor nodes. The number of chargers of *Minimum Energy* increases linearly since it deploys chargers for all sensor nodes. However, *Fewest Chargers for* C^3O, C^3OA and EC^3OA output the decreasing marginal returns of the number of chargers. This helps to reduce the increased deployment cost. Because EC^3OA has more positions to deploy chargers, it places fewest chargers.

As shown in Fig. 6(b), the energy consumption of all algorithms also increases. *Minimum Energy* can obtain the least energy consumption since there is no energy loss in charging. C^3OA also shows good performance in terms of energy consumption. Although its energy consumption is higher than that of *Minimum Energy*, it reduces 39.82% of energy consumption on average comparing with *Fewest Chargers for* C^3O. Because EC^3OA can choose more positions to deploy chargers, its energy consumption is less than that of C^3OA. We can see from Fig. 6(c) that C^3OA always performs well in terms of comprehensive cost. It reduces 25.3% and 9.85% of comprehensive cost on average comparing with *Minimum Energy* and *Fewest Chargers for* C^3O, respectively. Through

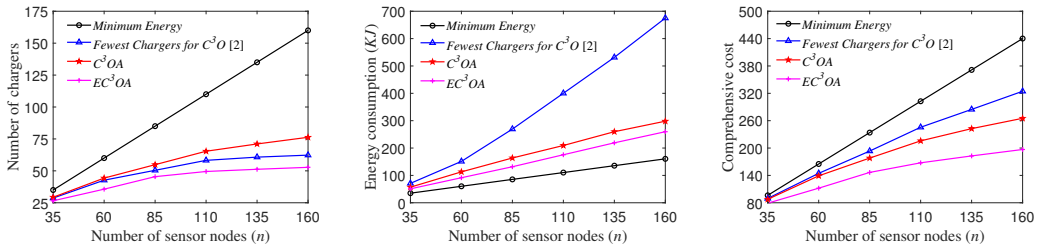

Fig. 6. Impact of number of sensor nodes. (a) Number of chargers. (b) Energy consumption. (c) Comprehensive cost.

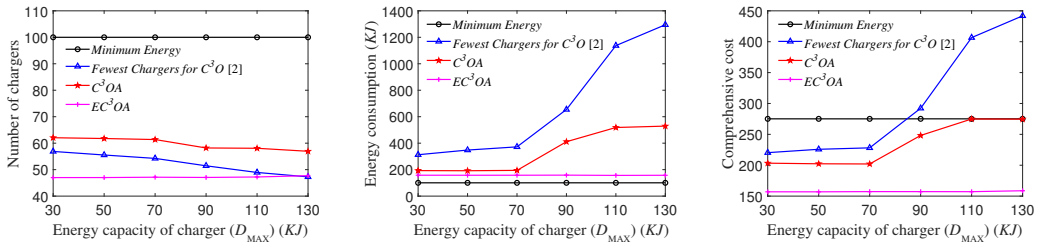

Fig. 7. Impact of energy capacity of charger. (a) Number of chargers. (b) Energy consumption. (c) Comprehensive cost.

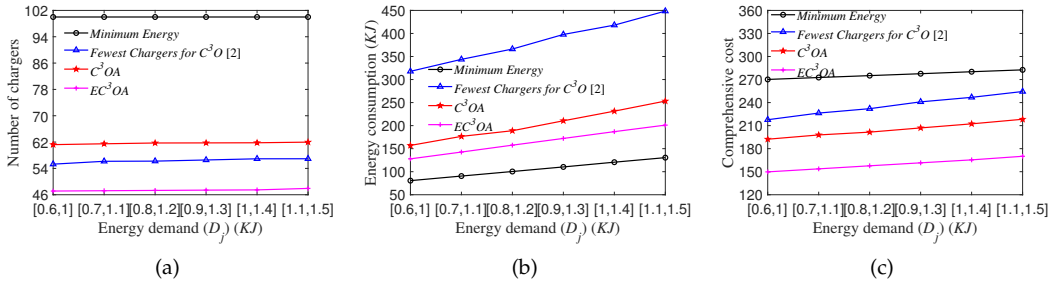

Fig. 8. Impact of energy demand of sensor node. (a) Number of chargers. (b) Energy consumption. (c) Comprehensive cost.

discretization, the comprehensive cost of EC^3OA is 19.93% lower than that of C^3OA on average.

7.4 Impact of Energy Capacity of Charger

We increase the energy capacity of charger from 30 to 130, and investigate the impact on different algorithms. As shown in Fig. 7(a), the number of chargers of *Fewest Chargers for* C^3O and C^3OA decreases with increasing energy capacity. And we can see from Fig. 7(b) that the energy consumption of *Fewest Chargers for* C^3O increases rapidly. This is because *Fewest Chargers for* C^3O construct larger charging trees, which consume more energy, when the energy capacity increases. C^3OA can determine the number of chargers flexibly based on the comprehensive cost, therefore, the energy consumption increases slowly. EC^3OA can keep the energy consumption low while maintaining a low number of chargers.

We can see from Fig. 7(c) that the comprehensive cost of *Fewest Chargers for* C^3O increases markedly. C^3OA reduces 14.86% and 19.15% of comprehensive cost on average comparing with *Minimum Energy* and *Fewest Chargers for* C^3O, respectively. Note that the change of energy capacity has no impact on *Minimum Energy* since the number of chargers does not change any more. Because EC^3OA can set chargers in better positions than in sensor nodes, it does not tend to choose the charging tree, of which the consumed energy close to energy capacity. Thus, the change of energy capacity has little impact on it. EC^3OA reduces 31.51% of comprehensive cost on average comparing with C^3OA.

7.5 Impact of Energy Demand of Sensor Nodes

We increase the energy demand of each sensor node from [0.6, 1] to [1.1, 1.5], and investigate the impact on four algorithms. As shown in Fig. 8(a), the number of chargers of *Minimum Energy* does not change because it deploys chargers for all sensor nodes. The numbers of chargers of other algorithms increase slightly. This is because when the charging demand is large, the charging trees become small, and more chargers are needed. When the charging trees are small enough, it is not necessary to add more chargers. As shown in Fig. 8(b), the energy consumption of all algorithms increases with increasing energy demand. This is because the energy consumption is proportional to the energy demand of sensor nodes. The energy consumption of *Fewest Chargers for* C^3O increases sharply because the energy loss of *Fewest Chargers for* C^3O is highest among all

This article has been accepted for publication in a future issue of this journal, but has not been fully edited. Content may change prior to final publication. Citation information: DOI 10.1109/TMC.2022.3162112, IEEE Transactions on Mobile Computing

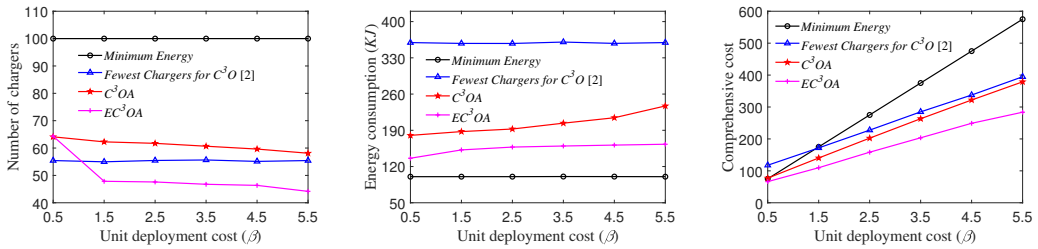

Fig. 9. Impact of unit deployment cost. (a) Number of chargers. (b) Energy consumption. (c) Comprehensive cost.

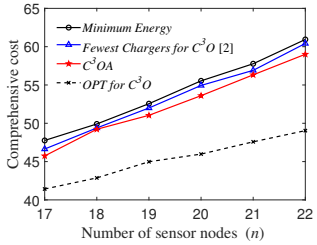

Fig. 10. Comparison with optimal solution.

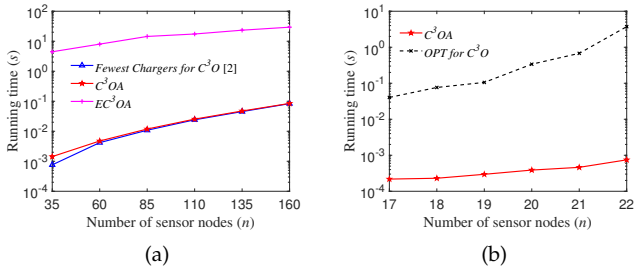

Fig. 11. Running time. (a) Large-scale simulations. (b) Small-scale simulations.

four algorithms. This means that *Fewest Chargers for* C^3O is unsuitable for the large energy demand situation.

We can see from Fig. 8(c), C^3OA reduces 25.9 % and 13.28 % of comprehensive cost comparing with *Minimum Energy* and *Fewest Chargers for* C^3O on average, respectively. EC^3OA reduces 22.06% of comprehensive cost on average comparing with C^3OA.

7.6 Impact of Unit Deployment Cost

Moreover, we change the unit deployment cost from 0.5 to 5.5 to simulate the possible market price relation between energy consumption and charger deployment. We can see from Fig. 9 that the numbers of chargers and energy consumption of *Minimum Energy* and *Fewest Chargers for* C^3O do not change since *Minimum Energy* always places charger for each sensor node, and *Fewest Chargers for* C^3O always constructs charging tree with the most sensor nodes. We can see from Fig. 9(a) that the numbers of chargers of C^3OA are gradually approaching to that of *Fewest Chargers for* C^3O. This is because that C^3OA will try to reduce the number of chargers to restrain the increase of comprehensive cost when the unit deployment cost increases. EC^3OA has more optional positions for charger placement, so the number of chargers decreases greatly. As shown in Fig. 9(b), the energy consumption of C^3OA is still much smaller than that of *Fewest Chargers for* C^3O, and the energy consumption of EC^3OA is less than that of C^3OA. Fig. 9(c) shows that C^3OA reduces 23.31% and 13.35% of comprehensive cost comparing with *Minimum Energy* and *Fewest Chargers for* C^3O on average, respectively. EC^3OA reduces 21.35% of comprehensive cost on average comparing with C^3OA.

7.7 Comparison with OPT for C^3O

There are infinite possible positions for the extended C^3O problem, and the optimal solution of extended C^3O problem can not be obtained. Therefore, we only consider the optimal solution for the original C^3O problem. We conduct a small-scale simulation in a square area $6m \times 6m$ to compare our algorithms with optimal solution of C^3O problem. In order to make the simulations more realistic, we change the coil radii from $0.12m$ to $0.08m$ to adapt to the small-scale environment. We find the optimal solution by enumerating all possible cases of charger deployment. Since we are searching the optimal charging forest, the number of edges will not exceed $n-1$ when the number of nodes is n. Assume that there are h edges in the graph $G(V,E)$, then the maximum number of edges in the charging forest is $w = \min\{h, n-1\}$. Without considering the energy constraint, there are at most $\sum_{z=0,1,\ldots,w} \binom{h}{z}$ charging forests. For a certain forest with z edges, the number of chargers is $n-z$, and we choose the locations of the chargers to minimize the energy consumption of the charging forest in order to minimize the comprehensive cost of the charging forest. By enumerating all cases, we discard the solutions that do not satisfy the energy constraint and then find the optimal one among the feasible solutions.

As shown in Fig. 10, we can see that C^3OA only increases 15.67% of the comprehensive cost comparing with *OPT for* C^3O on average. *Minimum Energy* and *Fewest Chargers for* C^3O increase 19.18% and 17.62% of the comprehensive cost comparing with *OPT for* C^3O on average, respectively.

7.8 Running Time

We conduct the large-scale simulations to compare the running time of *Fewest Chargers for* C^3O, C^3OA and EC^3OA and the small-scale simulations to compare the running time of C^3OA with that of *OPT for* C^3O. We do not consider the running time of *Minimum Energy*, because it does not need

time to calculate. In the larger-scale simulations, we can see from Fig. 11(a) that C^3OA can output the solution in 0.085 seconds when there are 160 sensor nodes, thus shows great expansibility. The running time of *Fewest Chargers for* C^3O is very close that of C^3OA after $n = 60$. Although EC^3OA shows great performance in the previous simulations, its running time is not ideal. When $n = 160$, the running time is 29.45 seconds. We can see from Fig. 11(b) that *OPT for* C^3O takes 3.7 seconds even for 22 sensor nodes. Although this time is only a few seconds, after analysis, it can be found that if n increases from 22 to 23, the number of edges will increase by 45 in the worst case. *OPT for* C^3O is based on the number of edges, which will lead to immeasurable huge time overhead. C^3OA is much faster than *OPT for* C^3O.

8 Discussion

So far, we have proposed a centralized algorithm C^3OA run on a central server to solve the C^3O problem. In this section, We discuss the distributed implement of C^3OA.

The basic idea is as follows. Each sensor node i receives neighbor information through local message exchange and executes Algorithm 2 to calculate the local $OCET$. Then, the best local $OCET$ can be obtained through local message exchange. The charging trees are constructed based on the best local $OCET$. Repeat the above process until all sensor nodes are covered by the charging trees.

To store the information of neighbors and itself, each sensor node i maintains a table and a local $OCET$ ${T^*}_i$. Here, the neighbors are the sensor nodes within the maximal communication range, which is larger than the maximal charging range generally. The table contains the information of i and its neighbors. There is a record for each sensor node j in the table, including the energy demand, position, coverage flag for indicating whether j is covered, and $cost_i(j)$ representing the average marginal comprehensive cost of ${T^*}_i$ when ${T^*}_i$ covers j.

To relieve the communication cost and avoid the complex communication protocol, all sensor nodes are clock-synchronized. Therefore, the distributed algorithm can be executed step by step. The major challenge is to avoid the "many to one" charging in the distributed way, i.e., each sensor node should be covered by only one charging tree. The distributed algorithm is executed on each sensor node i and follows the below stages.

Stage 1: Sensor node i sends its energy demand and position to its neighbors (Message 1). After receiving Message 1 from its neighbors, sensor node i initializes the table by setting the coverage flag as "uncovered" and $cost_i(j)$ as infinite for every j in the table. Moreover, set ${T^*}_i = \emptyset$.

Stage 2: According to current local $OCET$ ${T^*}_i$, sensor node i executes $EnPrim$ to cover the uncovered sensor nodes in local table, and the new local $OCET$ is termed $OCET$ ${T'^*}_i$. For all $j \in {V'^*}_i \backslash {V^*}_i$, let $cost_i(j) = \frac{F({T'^*}_i) - F({T^*}_i)}{|{V'^*}_i \backslash {V^*}_i|}$. Send all $cost_i(j)$, $j \in {V'^*}_i$, to its neighbors (Message 2).

Stage 3: Sensor node i receives Message 2 from neighbors and finds $j^* = \arg\min_j cost_j(i)$. Send the root j^* of best $OCET$ ${T'^*}_{j^*}$ covering i to its neighbors (Message 3).

Stage 4: Sensor node i receives Message 3 from neighbors. If all Message 3 indicate that i is the root of best $OCET$, i sends the message stating the sensor nodes in ${V'^*}_i$ have been covered to its neighbors (Message 4). If i is "uncovered", i marks itself as "covered", sets ${T^*}_i = {T'^*}_i$ and sends message stating i has been covered to its neighbors (Message 5).

Stage 5: If sensor node i receives Message 4 from neighbor j and $i \in {V'^*}_j$, i sends Message 5 and stops executing algorithm.

Stage 6: If sensor node i receives Message 5 from neighbor j, i marks j as "covered". If there is no uncovered sensor node in the table or no uncovered sensor node can be added to ${T^*}_i$, i stops executing algorithm. Otherwise, go to Stage 2.

Note that there must be at least one new local best $OCET$ that extends the previous local $OCET$ in each round, and at least one sensor node is covered by the new local best $OCET$ in each round. Finally, when all sensor nodes are covered, the distributed algorithm terminates. The final charging trees are the nonempty local $OCET$s stored in the sensor nodes. Obviously, the sensor nodes that sent Message 4 indicate the positions of chargers.

Next, we analyze the communication cost of distributed algorithm. During initialization, each sensor node i needs to send Message 1 once. In each iteration, if sensor node i is not covered by another tree, i must send Message 2 and Message 3. Only if its $OCET$ is determined, the sensor node sends the Message 4. If i is covered by its neighbor, it will send Message 5 once and stop executing algorithm. In the worst case, i needs to send all Message 2, Mesage 3 and Message 4 in each iteration. Since each iteration can cover at least one new sensor node, there are at most n iterations. Thus, i needs to send at most $3n$ messages in total. Message 1 and Message 5 are sent once in whole process. In summary, the total communication cost of any sensor node is $3n + 2$.

9 Conclusion

In this paper, we have defined a new metric, comprehensive cost, to measure the actual economic cost for charger deployment in multi-hop wireless charging. We have presented a multi-hop wireless charging model and formulated the C^3O problem to minimize the comprehensive cost with energy capacity constraints of chargers. The key contributions of this paper are proposing a $(\ln n + 1)$ - approximation algorithm for C^3O problem, a distributed algorithm for C^3O problem, a local cost sharing mechanism with desirable properties, two conflict avoidance schemes, and conducting simulations for evaluation. The key technical depth of this paper is in transforming the problem into weighted charging tree cover problem under the constraint of energy capacity, proposing the enhanced Prim algorithm to determine the optimal capacitated extension tree for each charging tree in polynomial time, proving the correctness of enhanced Prim algorithm, proving the approximation ratio for the designed algorithm, enabling the designed algorithm to be executed distributedly, showing the nonexistence of global *core* property and the inapplicability of *Shapley Value* method in cost sharing and proposing a local cost sharing mechanism satisfying the properties of local budget balance and local *core*. Our simulation results show that the proposed algorithms show significant superiority in terms of comprehensive cost.

ACKNOWLEDGMENTS

This work has been supported in part by the NSFC (No. 61872193, 61872191, 62072254).

REFERENCES

[1] X. Lu, P. Wang, D. Niyato, D. I. Kim, and Z. Han, "Wireless Charging Technologies: Fundamentals, Standards, and Network Applications," *IEEE Communications Surveys & Tutorials*, vol. 18, no. 2, pp. 1413-1452, 2016.

[2] C. Wang, J. Li, F. Ye, and Y. Yang, "A Novel Framework of Multi-Hop Wireless Charging for Sensor Networks Using Resonant Repeaters," *IEEE Transactions on Mobile Computing*, vol. 16, no. 3, pp. 617-633, 2017.

[3] J. O. Mur-Miranda, G. Fanti, Y. Feng, K. Omanakuttan, R. Ongie, A. Setjoadi, and N. Sharpe, "Wireless Power Transfer Using Weakly Coupled Magnetostatic Resonators," in *IEEE Energy Conversion Congress and Exposition*. IEEE, 2010, pp. 4179-4186.

[4] V. Kindl, R. Pechanek, M. Zavrel and T. Kavalir, "Inductive coupling system for E-bike wireless charging," in *2018 ELEKTRO*. IEEE, 2018, pp. 1-4.

[5] A. V. Sutar, V. Dighe, P. Karavkar, P. Mhatre, and V. Tandel, "Solar Energy based Mobile Charger Using Inductive Coupling Transmission," in *IEEE ICICCS*. IEEE, 2020, pp. 995-1000.

[6] H. Dai, K. Sun, A. X. Liu, L. Zhang, J. Zheng, and G. Chen, "Charging Task Scheduling for Directional Wireless Charger Networks," *IEEE Transactions on Mobile Computing*, vol. 20, no. 11, pp. 3163-3180, 2021.

[7] N. Wang, J. Wu, and H. Dai, "Bundle Charging: Wireless Charging Energy Minimization in Dense Wireless Sensor Networks," in *IEEE ICDCS*. IEEE, 2019, pp. 810-820.

[8] Y. Jin, J. Xu, S. Wu, L. Xu and D. Yang, "Enabling the Wireless Charging via Bus Network: Route Scheduling for Electric Vehicles," *IEEE Transactions on Intelligent Transportation Systems*, vol. 22, no. 3, pp. 1827-1839, 2021.

[9] M.K. Watfa, H. Al-Hassanieh, and S. Salmen, "The Road to Immortal Sensor Nodes," in *International Conference on Intelligent Sensors, Sensor Networks and Information Processing*. IEEE, 2009, pp. 523-528.

[10] W. X. Zhong, C. K. Lee, and S. Y. Hui, "Wireless Power Domino-Resonator Systems With Noncoaxial Axes and Circular Structures," *IEEE Transactions on Power Electronics*, vol. 27, no. 11, pp. 4750-4762, 2011.

[11] J. Xu, S. Hu, S. Wu, K. Zhou, H. Dai and L. Xu, "Cooperative Charging as Service: Scheduling for Mobile Wireless Rechargeable Sensor Networks," in *IEEE ICDCS*. IEEE, 2021, pp. 685-695.

[12] Y. Jin, J. Xu, S. Wu, L. Xu, D. Yang and K. Xia. "Bus network assisted drone scheduling for sustainable charging of wireless rechargeable sensor network," *Journal of Systems Architecture*, vol. 116, doi:10.1016/j.sysarc.2021.102059, 2021.

[13] *WiTricity*. Accessed: 2019. [Online]. Available: https://cn.comsol.com/story/download/350121/WiTricity_MS15.pdf

[14] T. Rault, A. Bouabdallah, and Y. Challal, "Multi-hop Wireless Charging Optimization in Low-Power Networks," in *IEEE Global Communications Conference*. IEEE, 2013, pp. 462-467.

[15] Y. Wu, Y. Feng, L. Guo, and X. Yang, "Deployment Method for Resonant Repeaters in Multi-hop Wireless Rechargeable Sensor Networks," *Transducer and Microsystem Technologies*, vol. 37, pp. 42-45+48, 2018.

[16] R. K. Ahuja, J. B. Orlin, S. Pallottino, M. P. Scaparra, and M. G. Scutellà, "A Multi-Exchange Heuristic for the Single-Source Capacitated Facility Location Problem," *Management Science*, vol. 50, no. 6, pp. 749-760, 2004.

[17] Y. Ma, W. Liang and W. Xu, "Charging Utility Maximization in Wireless Rechargeable Sensor Networks by Charging Multiple Sensors Simultaneously," *IEEE/ACM Transactions on Networking*, vol. 26, no. 4, pp. 1591-1604, 2018.

[18] Y. Peng, Z. Li, W. Zhang and D. Qiao, "Prolonging Sensor Network Lifetime Through Wireless Charging," in *IEEE Real-Time Systems Symposium*. IEEE, 2010, pp. 129-139.

[19] Y. Shi, L. Xie, Y. T. Hou and H. D. Sherali, "On renewable sensor networks with wireless energy transfer," in *IEEE INFOCOM*. IEEE, 2011, pp. 1350-1358.

[20] P. Zhou, C. Wang and Y. Yang, "Self-sustainable Sensor Networks with Multi-source Energy Harvesting and Wireless Charging,"in *INFOCOM*. IEEE, 2019, pp. 1828-1836.

[21] C. Wang, J. Li, Y. Yang and F. Ye, "Combining Solar Energy Harvesting with Wireless Charging for Hybrid Wireless Sensor Networks," *IEEE Transactions on Mobile Computing*, vol. 17, no. 3, pp. 560-576, 2018.

[22] S. Li, J. He, X. Zhang, and J. Peng, "An Energy Efficient Multi-hop Charging Scheme with Mobile Charger for Wireless Rechargeable Sensor Network," in *International Conference on Algorithms & Architectures for Parallel Processing*. Springer, 2015, pp. 648-660.

[23] S. Tragantalerngsak, J. Holt, and M. Rönnqvist, "An Exact Method for the Two-echelon, Single-source, Capacitated Facility Location Problem," *European Journal of Operational Research*, vol. 123, no. 3, pp. 473-489, 2000.

[24] S.Tragantalerngsak, J. Holt, and M. Rönnqvist, "Lagrangian Heuristics for the Two-echelon, Single-source, Capacitated Facility Location Problem," *European Journal of Operational Research*, vol. 102, no. 3, pp. 611-625, 1997.

[25] P. Yang, T. Wu, H. Dai, X. Rao, X. Wang, P. Wan, and X. He, "MORE: Multi-node Mobile Charging Scheduling for Deadline Constraints," *ACM Transactions on Sensor Networks*, vol. 17, no. 1, pp. 1-21, 2020.

[26] K. Jain and M. Mahdian, "Cost Sharing," *Algorithmic Game Theory*, N. Nisan, T. Roughgarden, E. Tardos, and V. V. Vazirani (Eds.). Cambridge Univ, Cambridge, U.K., 2007.

[27] T. Ichiishi, "For a Proof of Unique Existence," *Game Theory for Economic Analysis*. Academic, New York, pp. 118–120, 2014.

[28] D. J. A. Welsh and M. B. Powell, "An upper bound for the chromatic number of a graph and its application to timetabling problems," *Computer Journal*, vol. 10, no. 1, pp. 85-86, 1967.

[29] J. Meditch and C. Lea, "Stability and Optimization of the CSMA and CSMA/CD Channels," *IEEE Transactions on Communications*, vol. 31, no. 6, pp. 763-774, 1983.

[30] B. Kwak, N. Song and L. E. Miller, "Performance analysis of exponential backoff," *IEEE/ACM Transactions on Networking*, vol. 13, no. 2, pp. 343-355, 2005.

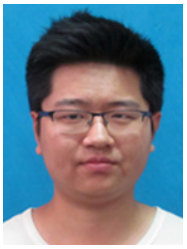

Sixu Wu received the bachelor's degree in School of Computer Science from Nanjing University of Posts and Telecommunications, Jiangsu, China, in 2019. He is currently a doctoral student in the School of Computer Science at Nanjing University of Posts and Telecommunications. His main research interest is wireless rechargeable sensor network.

Haipeng Dai (M'14) received the B.S. degree in the Department of Electronic Engineering from Shanghai Jiao Tong University, Shanghai, China, in 2010, and the Ph.D. degree in the Department of Computer Science and Technology in Nanjing University, Nanjing, China, in 2014. His research interests are mainly in the areas of data mining, Internet of Things, and mobile computing. He is an associate professor in the Department of Computer Science and Technology in Nanjing University. His research papers have been published in many prestigious conferences and journals such as ACM VLDB, IEEE ICDE, ACM SIGMETRICS, ACM MobiSys, ACM MobiHoc, ACM UbiComp, IEEE INFOCOM, IEEE ICDCS, IEEE ICNP, IEEE SECON, IEEE IPSN, IEEE JSAC, IEEE/ACM TON, IEEE TMC, IEEE TPDS, IEEE TDSC, and IEEE TOSN. He is an IEEE and ACM member. He serves/ed as Poster Chair of the IEEE ICNP'14, Track Chair of the ICCCN'19 and the ICPADS'21, TPC member of the ACM MobiHoc'20-21, IEEE INFOCOM'20-22, IEEE ICDCS'20-21, IEEE ICNP'14, IEEE IWQoS'19-21, IEEE IPDPS'20'22 and IEEE MASS'18-19. He received Best Paper Award from IEEE ICNP'15, Best Paper Award Runner-up from IEEE SECON'18, and Best Paper Award Candidate from IEEE INFOCOM'17.

Lijie Xu received his Ph.D. degree in the Department of Computer Science and Technology from Nanjing University, Nanjing, in 2014. He was a research assistant in the Department of Computing at the Hong Kong Polytechnic University, Hong Kong, from 2011 to 2012. He is currently an associate professor in the School of Computer Science at Nanjing University of Posts and Telecommunications, Nanjing. His research interests are mainly in the areas of wireless sensor networks, ad-hoc networks, mobile and distributed computing, and graph theory algorithms.

Linfeng Liu (M'13) received the B. S. and Ph. D. degrees in computer science from the Southeast University, Nanjing, China, in 2003 and 2008, respectively. At present, he is a Professor in the School of Computer Science and Technology, Nanjing University of Posts and Telecommunications, China. His main research interests include the areas of vehicular ad hoc networks, wireless sensor networks and multi-hop mobile wireless networks. He has published more than 80 peer-reviewed papers in some technical journals or conference proceedings, such as IEEE TMC, IEEE TPDS, ACM TAAS, IEEE TSC, IEEE TVT, IEEE IoTJ, Computer Networks, Elsevier JPDC.

Fu Xiao (M'12) received the Ph.D. degree in computer science and technology from the Nanjing University of Science and Technology, Nanjing, China, in 2007. He is currently a Professor in the School of Computer Science, Nanjing University of Posts and Telecommunications. His main research interests are wireless sensor networks and mobile computing. He is a member of the IEEE Computer Society and the Association for Computing Machinery.

Jia Xu (M'15, SM'21) received the M.S. degree in School of Information and Engineering from Yangzhou University, Jiangsu, China, in 2006 and the PhD. Degree in School of Computer Science and Engineering from Nanjing University of Science and Technology, Jiangsu, China, in 2010. He is currently a professor in the School of Computer Science at Nanjing University of Posts and Telecommunications. He was a visiting Scholar in the Department of Electrical Engineering & Computer Science at Colorado School of Mines from Nov. 2014 to May. 2015. His main research interests include crowdsourcing, edge computing and wireless sensor networks. Prof. Xu has served as the PC Co-Chair of SciSec 2019, Publicity Co-Chair of SciSec 2021 and SciSec 2022, Organizing Chair of ISKE 2017, TPC member of IEEE Globecom, IEEE ICC, IEEE MASS, IEEE ICNC, and IEEE EDGE.